OPTIMAL CONTROL OF MELT SPINNING PROCESSES

T. GÖTZ AND S.S.N. PERERA

ABSTRACT. An optimal control problem for a mathematical model of a melt spinning process is considered. Newtonian and non–Newtonian models are used to describe the rheology of the polymeric material, the fiber is made of. The extrusion velocity of the polymer at the spinneret as well as the velocity and temperature of the quench air serve as control variables. A constrained optimization problem is derived and the first–order optimality system is set up to obtain the adjoint equations. Numerical solutions are carried out using a steepest descent algorithm.

Keywords: Fiber spinning, Optimal control, First–order optimality system, Adjoint system

1. Introduction

Many kinds of synthetic textile fibers, like Nylon, Polyester, etc. are manufactured by a so–called melt spinning process. In this process, the molten polymer is extruded through a die called the spinneret to create a slender, cylindrical jet of viscous polymer, the fiber. Far away from the spinneret, the fiber is wrapped around a drum, which pulls it away at a pre–determined take–up speed. The take–up speed is much higher than the extrusion speed; in industrial processes the take–up speed is about 50m/s and the extrusion speed is about 10m/s, see [2, 6]. The ratio between the take–up speed v_L and the extrusion speed v_0 is called draw–ratio $d = v_L/v_0 > 1$. Hence the filament is stretched considerably in length and therefore it decreases in diameter. The ambient atmosphere temperature is below the polymer solidification temperature such that the polymer is cooled and solidifies before the take–up, see Figure 1. In industrial processes a whole bundle of hundreds of single filaments is extruded and spun in parallel, however for the analysis we consider a single filament.

The dynamics of melt spinning processes has been studied by many research groups throughout the world during the last decades starting with early works of Kase and Matsuo [4] and Ziabicki [10]. In later works, the energy balance for the heat transfer was introduced into the model, and more and more sophisticated descriptions, including material effects, crystallization kinetics and viscoelastic behavior, were developed by several authors in order to achieve a better understanding of the fiber formation process. Up to now it is possible to use the basic models with more or less modifications in different technological aspects of the melt spinning process. Due to the complex behaviour of the polymeric material, several parameters are included in all the available models. Typically, these parameters are hard to

Date: January 17, 2008.

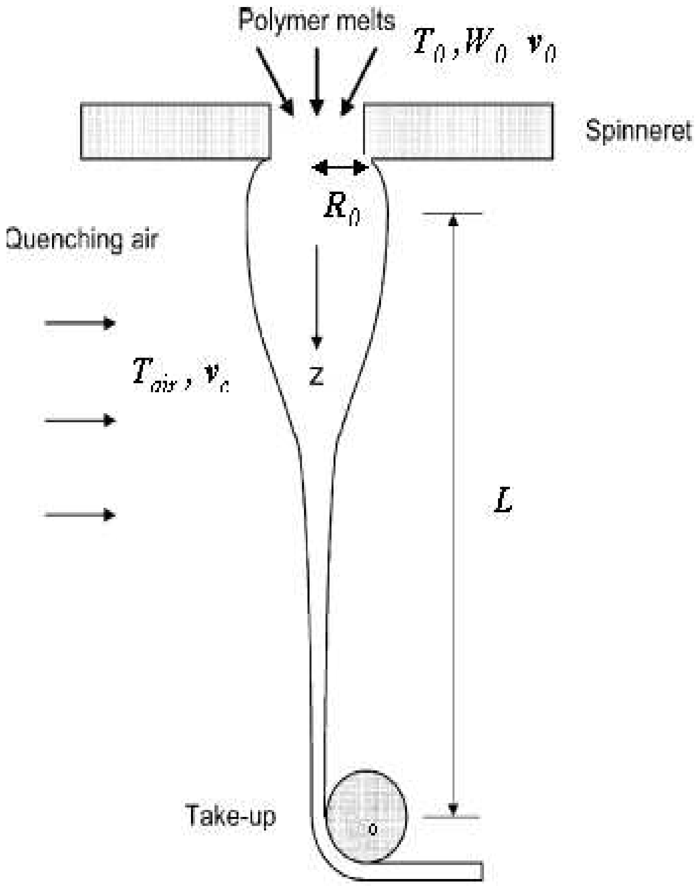

FIGURE 1. Sketch of the melt spinning process.

measure. An identification based on comparing available data and simulations is one way to determine those parameters. Additionally, the outcome of the melt spinning process depends heavily on the boundary conditions, e.g. the draw ratio, the ambient temperature, the quench air velocity and temperature. The question of optimizing the fiber production with respect to the external variables has not yet been treated in the literature.

The main goal of this study is to optimize the melt spinning process with respect to the final temperature, the quench air velocity and temperature. To model the fiber spinning process, we consider both a Newtonian model for the viscosity and a non–Newtonian model, where the viscosity is temperature–dependent. We formulate the optimal control problem as a constrained minimization problem, see [3], and derive formally the corresponding first–order optimality system via the Lagrange functional. For the numerical computation of the optimal control variables we present a steepest descent algorithm using the adjoint variables.

The paper is organized as follows. In Section 2, we present the models and define the cost functional which ought to be minimized. In Section 3, the first–order optimality system is derived. The steepest descent algorithm is discussed in Section 4. Finally, some numerical results are presented in Section 5 and concluding remarks can be found in Section 6.

2. The Optimal Control Problem

2.1. **Melt Spinning Model.** Considering the basic conservation laws for mass, momentum and energy of the viscous polymer jet one can obtain by averaging over the cross–section of the slender fiber the following set of equations, see [6, 7, 8].

$$\rho A v = W_0 \ . \tag{1a}$$

$$\rho A v \frac{dv}{dz} = \frac{dA\tau}{dz} - \sqrt{A\pi} C_d \rho_{air} v^2 + \rho A g \ , \tag{1b}$$

$$\rho C_p v \frac{dT}{dz} = -\frac{2\alpha\sqrt{\pi}}{\sqrt{A}}(T - T_\infty) \ , \tag{1c}$$

In the mass balance (1a), A denotes the cross–sectional area of the fiber, v is the velocity of the fiber along the spinline and W_0 equals the mass flux through the spinneret. The density ρ of the polymer is assumed to be constant. In the momentum balance (1b), z denotes the coordinate along the spinline, g is the gravitational acceleration and C_d is the air drag coefficient. The axial stress τ is related via the constitutive equation

$$\tau = 3\eta \frac{dv}{dz} \tag{1d}$$

to the viscosity η. In the energy equation (1c), T and C_p denote the temperature and the heat capacity of the polymer, T_∞ is the temperature of the quench air and α denotes the heat transfer coefficient between the fiber and the quench air.

According to [6], we assume the following relations for the air drag coefficient

$$C_d = 0.37 \, \mathrm{Re}_{\mathrm{air}}^{-0.61}$$

and the heat transfer coefficient

$$\alpha = \frac{0.21}{R_0} \kappa \mathrm{Re}_{\mathrm{air}}^{\frac{1}{3}} \left[1 + \frac{64 v_c^2}{v^2} \right]^{\frac{1}{6}}$$

depending on the Reynolds–number of the quench air flow

$$\mathrm{Re}_{\mathrm{air}} = \frac{2 v \rho_{\mathrm{air}}}{\eta_{\mathrm{air}}} \sqrt{\frac{A}{\pi}} \ .$$

Here R_0 is the radius of the spinneret, $\rho_{\mathrm{air}}, \eta_{\mathrm{air}}$ and κ represent the density, viscosity and heat conductivity of the air and v_c is the velocity of the quench air.

In the Newtonian model, the viscosity $\eta = \eta_0$ of the polymer is constant, whereas in the non–Newtonian case, we consider an Arrhenius–type temperature dependence

$$\eta = \eta_0 \exp\left[\frac{E_a}{R_G}\left(\frac{1}{T} - \frac{1}{T_0}\right)\right]. \tag{1e}$$

where $\eta_0 > 0$ is the zero shear viscosity at the initial temperature T_0, E_a denotes the activation energy and R_G equals to the gas constant.

The equations (1a)—(1c) are subject to the boundary conditions

$$v = v_0 \quad \text{and} \quad T = T_0 \qquad \text{at } z = 0 \tag{1f}$$

$$v = v_L \qquad \text{at } z = L \tag{1g}$$

where L denotes the length of the spinline.

2.2. **Dimensionless Form.** Introducing the dimensionless quantities

$$v^* = \frac{v}{v_0}\,, \quad z^* = \frac{z}{L}\,, \quad T^* = \frac{T}{T_0}\,, \quad A^* = \frac{A}{A_0} \quad \text{and} \quad q^* = \frac{q}{q_0}\,,$$

where $q = \frac{\rho A \tau}{W_0}$ and $q_0 = \frac{\rho A_0 v_0 \eta_0}{L W_0}$, the system (1) can be formulated in dimensionless form. Dropping the star, the system reads as

$$\frac{dv}{dz} = \frac{qv}{3\eta}\,, \tag{2a}$$

$$\frac{dq}{dz} = \mathrm{Re}\left(\frac{qv}{3\eta} - \frac{\mathrm{Fr}^{-1}}{v} + Cv^{3/2}\right)\,, \tag{2b}$$

$$\frac{dT}{dz} = -\gamma\frac{T - T_\infty}{\sqrt{v}}\,, \tag{2c}$$

where $\mathrm{Re} = \frac{\rho L v_0}{\eta_0}$ is the Reynold number, $\mathrm{Fr}^{-1} = \frac{gL}{v_0^2}$ is the inverse of the Froude number, $C = \frac{C_d \rho_{\mathrm{air}} L}{\rho R_0}$ is the scaled drag coefficient and $\gamma = \frac{2\alpha L}{\rho C_p v_0 R_0}$ denotes the scaled heat transfer coefficient.

The viscosity is given by

$$\eta = \begin{cases} 1 & \text{for the Newtonian model} \\ \exp\left[\frac{E_a}{R_G T_0}\left(\frac{1}{T} - 1\right)\right] & \text{for the non–Newtonian model.} \end{cases} \tag{2d}$$

The boundary conditions read as

$$v(0) = 1 \quad \text{and} \quad T(0) = 1\,, \tag{2e}$$

$$v(1) = d \tag{2f}$$

where $d = v_L/v_0 > 1$ denotes the draw–ratio.

2.3. **Cost Functional.** We want to control the temperature profile of the fiber, such that the final temperature $T(1)$ is below the solidification point $T_s^* = T_s/T_0$. On the other hand we want to maximize the outflow, i.e. maximize v_0. The air temperature T_∞ and the air velocity v_c can be influenced and hence serve as control variables. Therefore, we consider the following cost functional

$$\begin{aligned} J = J(y,u) &= J_1 + J_2 + J_3 + J_4 \\ &= -\omega_1 u_3 + \omega_2 (y_3(1) - T_s^*) \\ &\quad + \frac{\omega_3}{2} \int_0^1 (u_2(z) - T_{\text{ref}})^2 dz + \frac{\omega_4}{2} \int_0^1 u_1(z)^2 dz \end{aligned} \tag{3}$$

where $y = (v, q, T) \in Y$ denotes the vector of state variables and $u = (v_c, T_\infty, v_0) \in U$ are the controls. The weighting coefficients $\omega_i > 0$, $i = 1 \dots 4$ allow to adjust the cost functional to different scenarios.

Summarizing, we consider the following constrained optimization problem

$$\text{minimize } J(y,u) \text{ with respect to } u, \text{ subject to (2)} \tag{4}$$

In the sequel, we will address this problem using the calculus of adjoint variables.

3. The First–Order Optimality System

In this section we introduce the Lagrangian associated to the constrained minimization problem (4) and derive the system of first–order optimality conditions.

Let $Y = C^1([0,1];\mathbb{R}^3)$ be the state space consisting of triples of differentiable functions $y = (v, q, T)$ denoting velocity, stress and temperature of the fiber. Further, let $U = C^1([0,1];\mathbb{R}^2) \times \mathbb{R}$ be the control space consisting of a pair $(u_1, u_2) = (v_c, T_\infty)$ of differentiable functions, i.e. air velocity and temperature, and a scalar $u_3 = v_0$ interpreted as the inflow velocity.

We define the operator $e = (e_v, e_q, e_T) : Y \times U \to Y^*$ via the weak formulation of the state system (2):

$$\langle e(y,u), \xi \rangle_{Y,Y^*} = 0 \qquad \forall \xi \in Y^*$$

where $\langle \cdot, \cdot \rangle_{Y,Y^*}$ denotes the duality pairing between Y and its dual space Y^*. Now, the minimization problem (4) reads as

$$\text{minimize } J(y,u) \text{ with respect to } u \in U, \text{ subject to } e(y,u) = 0.$$

Introducing the Lagrangian $\mathcal{L} : Y \times U \times Y^* \to \mathbb{R}$ defined as

$$\mathcal{L}(y,u,\xi) = J(y,u) + \langle e(y,u), \xi \rangle_{Y,Y^*} \ ,$$

the first–order optimality system reads as

$$\nabla_{y,u,\xi} \mathcal{L}(y,u,\xi) = 0 \ .$$

Considering the variation of $\mathcal{L}$ with respect to the adjoint variable ξ, we recover the state system

$$e(y,u) = 0$$

or in the classical form

$$\frac{dy}{dz} = f(y,u) \ , \quad \text{with } v(0) = 1,\ v(1) = d,\ T(0) = 1 \tag{5}$$

where

$$f(y,u) = \begin{pmatrix} \frac{qv}{3\eta} \\ \mathrm{Re}\left(\frac{qv}{3\eta} - \frac{\mathrm{Fr}^{-1}}{v} + Cv^{3/2}\right) \\ -\gamma \frac{T-T_\infty}{\sqrt{v}} \end{pmatrix} .$$

Second, taking variations of $\mathcal{L}$ with respect to the state variable y we get the adjoint system

$$J_y(y,u) + e_y^*(y,u)\xi = 0$$

or in classical form

$$-\frac{d\xi}{dz} = F(y,u,\xi) , \quad \text{with } \xi_q(0) = 0,\ \xi_q(1) = 0,\ \xi_T(1) = -\omega_2 , \tag{6}$$

where

$$F(y,u,\xi) = \left(\frac{\partial f}{\partial y}\right)^\top \xi .$$

Finally, considering variations of $\mathcal{L}$ with respect to the control variable u in a direction of δu we get the optimality condition

$$\langle J_u(y,u), \delta u\rangle + \langle e_u(y,u)\delta u, \xi\rangle = 0 . \tag{7}$$

In the optimum, this holds for all $\delta u \in U$.

4. Algorithm

To solve the nonlinear first–order optimality system (5), (6) and (7), we propose an iterative steepest–descent method.

(1) *Set $k = 0$ and choose initial control $u^{(0)} \in U$.*
(2) *Given the control $u^{(k)}$. Solve the state system* (5) *with a shooting method to obtain $y^{(k+1)}$.*
(3) *Solve the adjoint system* (6) *with a shooting method to obtain $\xi^{(k+1)}$.*
(4) *Compute the gradient $g^{(k+1)}$ of the cost functional*
(5) *Update the control $u^{(k+1)} = u^{(k)} - \beta g^{(k+1)}$ for a step size $\beta > 0$.*
(6) *Compute the cost functional $J^{(k+1)} = J(y^{(k+1)}, u^{(k+1)})$.*
(7) *If $\left|J^{(k+1)} - J^{(k)}\right| \geq Tol$, goto 2.*

Here, Tol is some prescribed tolerance for the termination of the optimization procedure. In each iteration step, we need to solve two boundary value problems, i.e. the state system (5) and the adjoint system (6) in the step 2 and 3 of the algorithm. Both systems are solved using a shooting method based on a Newton–iteration.

4.1. Shooting Method.

Now, we present the main steps of the shooting method for the state system (5) in particulary. Let us make an initial guess s for $y_2(0)$ and denote by $y(z; s)$ the solution of the initial value problem

$$\frac{dy}{dz} = f(y,u) , \quad \text{with } y_1(0) = 1,\ y_2(0) = s,\ y_3(0) = 1 . \tag{8}$$

Now we introduce new dependent variables

$$x(z;s) = \frac{\partial y}{\partial s}$$

and define second system as follows

$$\frac{\partial x}{\partial z} = \left(\frac{\partial f}{\partial y}\right) x \quad \text{with} \quad x_1(0;s) = 0,\ x_2(0;s) = 1,\ x_3(0;s) = 0. \tag{9}$$

The solution of $y(z;s)$ of the initial value problem (8) coincides with the solution $y(z)$ of the boundary value state system (5) provided that the value s can be found such that

$$\phi(s) = y_1(1;s) - d = 0.$$

Using the system (9), $\phi'(s)$ can be computed as follows

$$\phi'(s) = x_1(1;s).$$

Now, using Newton–iteration a sequence $(s_n)_{n\in\mathbb{N}}$ is generated by

$$s_{n+1} = s_n - \frac{\phi(s_n)}{\phi'(s_n)} \quad \text{for a given initial guess } s_0.$$

If the initial guess s_0 is a sufficiently good approximation to the required root of $\phi(s) = 0$ the theory of the Newton–iteration method ensures that the sequence $(s_n)_{n\in\mathbb{N}}$ converges to the root s.

4.2. **Step Size Control with Polynomial Models.** Crucial for the convergence of the algorithm is the choice of the step size β (in step 5 of the algorithm) in the direction of the gradient. Clearly, the best choice would be the result of a line search

$$\beta^* = \operatorname{argmin}_{\beta>0} J(u_k - \beta d_k).$$

However this is numerically quite expensive although it is a one dimensional minimization problem. Instead of the exact line search method, we use an approximation based on a quadratic polynomial method [5] in order to find β^* such that which minimize $J(u_k - \beta d_k)$. We construct quadratic polynomial for

$$\Phi(\beta) = J_1(u_k - \beta d_k),$$

using following data points,

$$\Phi(0) = J_1(u_k), \quad \Phi(1) = J_1(u_k - d_k), \quad \Phi'(0) = \nabla\Phi(u_k)^{\mathrm{T}} d_k < 0.$$

Then the quadratic polynomial of β reads as follows,

$$\Lambda(\beta) = \Phi(0) + \Phi'(0)\beta + (\Phi(1) - \Phi(0) - \Phi'(0))\beta^2.$$

The global minimum of Φ is ,

$$\beta^* = \frac{-\Phi'(0)}{2(\Phi(1) - \Phi(0) - \Phi'(0))} \in (0,1).$$

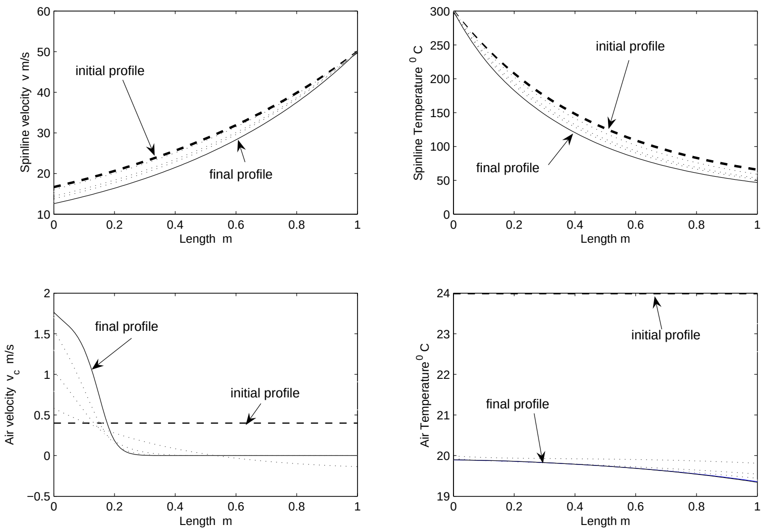

FIGURE 2. Spinline velocity (up-left) and temperature (up-right) profile, initial (dash) after optimization (solid) and intermediate (dot). Air velocity (down-left) and temperature (down-right) profile, initial (dash) after optimization (solid) and intermediate (dot).

4.3. **Numerics.** Both state and adjoint system of ODE were solved using the Matlab routine ode23tb. This routine uses an implicit method with backward differentiation to solve stiff differential equations. It is an implementation of TR-BDF2 [9], an implicit two stage Runge-Kutta formula where the first stage is a trapezoidal rule step and the second stage is a backward differentiation formula of order two.

5. Results

5.1. **Newtonian Model.** Figure 2 shows spinline velocity, temperature and air velocity, temperature profiles before optimization and after optimization for Newtonian model. It also shows some of intermediate profiles. Corresponding cost functional is shown in figure 3. In this case we use $\omega_1 = 1, \omega_2 = 1, \omega_3 = 1.5$ and $\omega_1 = 2.5$.

It can be seen that in an optimal state final temperature is below 50°C. The extrusion velocity drops from 16.67 m/s to 12.65 m/s. Optimal air temperature profile is more or less close to 20°C which we considered as a reference temperature. In this case optimal air velocity profile is very high near the spinneret exit point and beyond 30 cm from spinneret exit point it almost equals to zero.

Figure 4 visualizes the optimal air velocity and air temperature profiles in Newtonian model for different weighting coefficients.

5.2. **Non-Newtonian Model.** Figure 5 visualizes spinline velocity, temperature and air velocity, temperature profiles before optimization and after

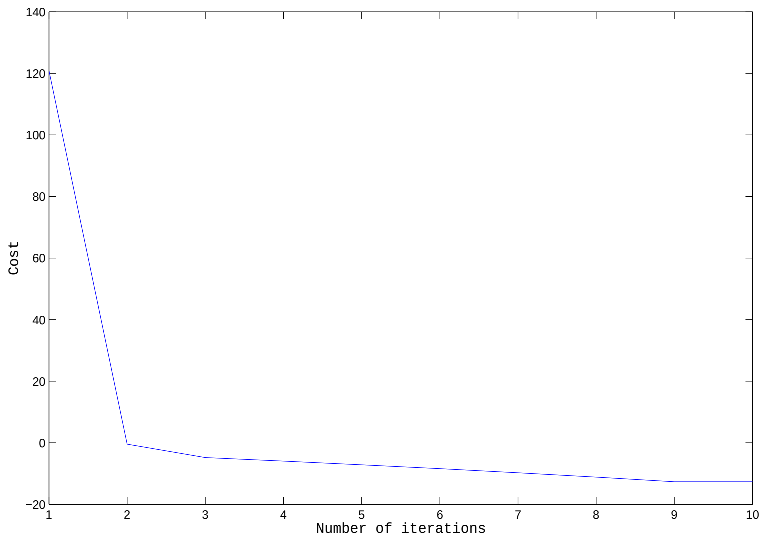

FIGURE 3. Cost functional Newtonian model.

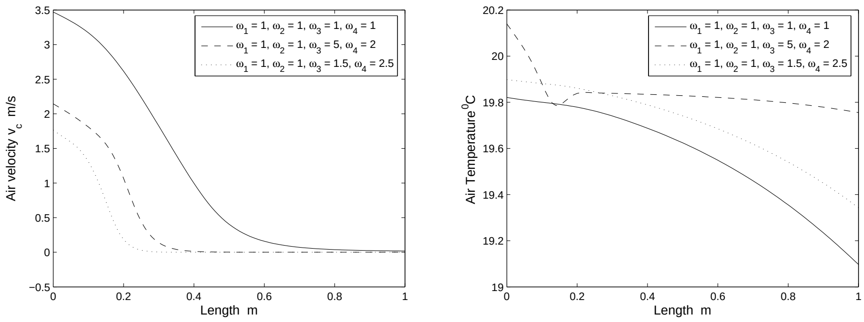

FIGURE 4. Optimal air velocity (left), air temperature (right) profiles in Newtonian model for different weighting coefficients.

optimization for Non-Newtonian model. Corresponding cost functional is shown in figure 7. Here we use $\omega_1 = 1, \omega_2 = 1, \omega_3 = 1.5$ and $\omega_1 = 2.5$.

Likes Newtonian model, in the optimal state final temperature is below 50°C and optimal air temperature profile is more or less close to 20°C. The extrusion velocity drops from 16.67 m/s to 10.42 m/s. In the optimal state, the air velocity gets high value near the spinneret exit point and just after this point it almost close to zero.

Figure 6 shows optimal air velocity and air temperature profile in non-Newtonian model for different cost coefficients.

6. Conclusions

We studied an optimal control problem for a melt spinning process. The aim was to maximize the outflow, minimize the air velocity and air

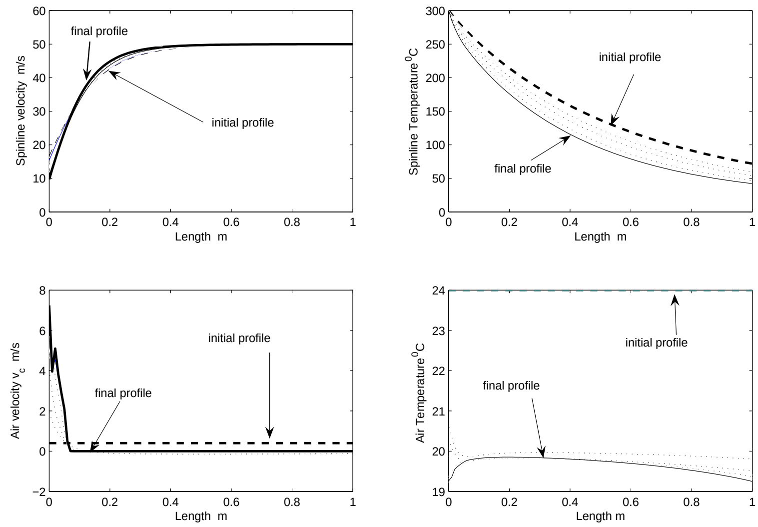

FIGURE 5. Spinline velocity (up-left) and temperature (up-right) profile, initial (dash) after optimization (solid) and intermediate (dot). Air velocity (down-left) and temperature (down-right) profile, initial (dash) after optimization (solid) and intermediate (dot).

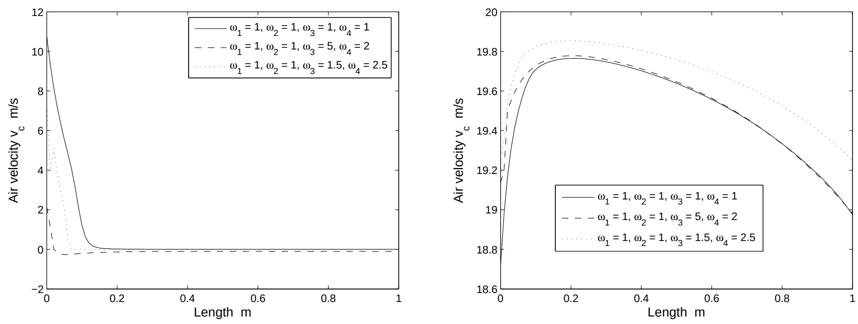

FIGURE 6. Optimal air velocity (left), air temperature (right) profiles in non-Newtonian model for the different weighting coefficients.

temperature and get final spinline temperature below fiber solidification temperature. Here, Newtonian and Non-Newtonian models were considered. Defining the cost functional we converted this problem into the constrained optimization problem and derived the first order optimality system. For the numerical solution we proposed steepest descent algorithm based on adjoint variable method. For the step size control, polynomial type model was considered. Different cost coefficients were considered in both cases.

In an optimal profile, final temperature was below 50°C in both models where the air temperature is also reduced to more or less equal to 20°C

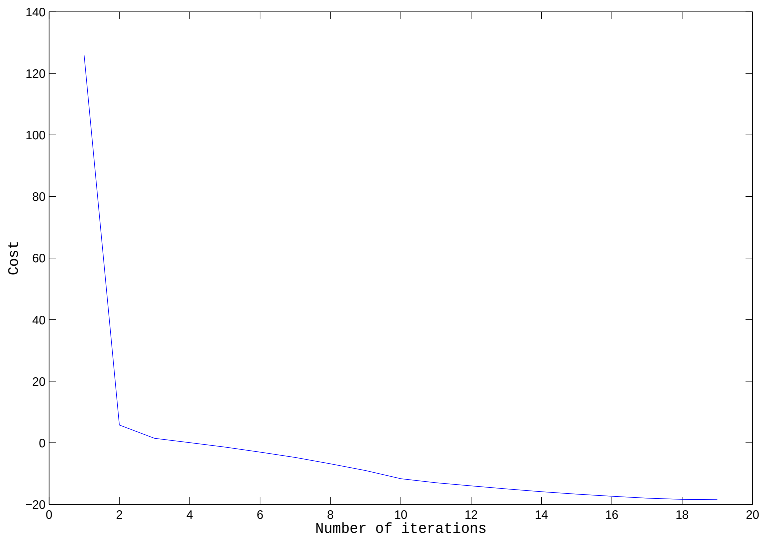

FIGURE 7. Cost functional Non-Newtonian model.

(which we used as a reference temperature). Concerning air velocity, both cases need it only initially (up to 0.2 m). It can be noticed both cases initial velocity decreased. Clearly, this is success concerning the cost.

Acknowledgements: The research of S.S.N. Perera was supported by a grant from the DAAD (German Academic Exchange Services).

REFERENCES

[1] Bird RB, Amstrong RC, Hassager O (1987) Dynamics of Polymeric Liquids. 2^{nd} edition, Volume 1: Fluid Mechanics, John Wiley & Sons.
[2] Brünig H, Roland H, Blechschmidt D (1997) High Filament Velocities in the Underpressure Spunbonding Nonwoven Process. IFJ:129-134, December 1997.
[3] Ito K, Ravindran SS (1998) Optimal control of thermally convected fluid flows. SIAM J. Sci. Comput., 19(6):1847-1869.
[4] Kase S, Matsuo T (1965) Studies on Melt Spinning, Fundermental Equations on the Dynamics of Melt Spinning. J. Polym. Sci. Part A 3: 2541-2554.
[5] Kelley CT (1999) Iterative Methods for Optimization. SIAM.
[6] Langtangen HP (1997) Derivation of a Mathematical Model for Fiber Spinning. Department of Mathematics, Mechanics Division, University of Oslo, December 1997.
[7] Lee JS, Jung HW, Hyun JC, Seriven LE (2005) Simple Indicator of Draw Resonance Instability in Melt Spinning Processes. AIChE Journal, Vol. 51, No. 10:2869-2874.
[8] Lee JS, Shin DM, Jung HW, Hyun JC (2005) Transient Solution of the Dynamics in Low-Speed Fiber Spinning Process Accompanied by Flow-included Crystallization. J. Non-Newtonian Fluid Mech. 130:110-116.
[9] Shampine LF, Reichelt MW (1997) The MATLAB ODE Suite. SIAM Journal of Scientific Computing, Vol: 18:1-22.
[10] Ziabicki A (1976) Fundermentals of Fiber Formation. Wiley-Interscience, New York.

T. Götz, Department of Mathematics, University of Kaiserslautern, Postbox 3049, D-67653 Kaiserslautern, Germany. E–Mail goetz@mathematik.uni-kl.de

S.S.N. Perera, Department of Mathematics, University of Kaiserslautern, Postbox 3049, D-67653 Kaiserslautern, Germany. E–Mail perera@mathematik.uni-kl.de